

Calibration of a Digital Phased Array for Polarimetric Radar

Caleb Fulton and William J. Chappell

Purdue University, West Lafayette, Indiana, 47906, USA

Abstract — When an active phased array is used for polarimetric radar applications, the system must be calibrated to reflect the fact that polarization of the transmitted and received fields is dependent on the scan angle. This paper discusses the challenges of polarimetric phased array calibration, and demonstrates these techniques using a linear array of eight S-band dual-polarized antennas connected to an active Digital Array Radar (DAR) prototype system. The ability to accurately measure polarimetric scattering matrices is demonstrated after using direct far-field measurements to compensate for polarization errors on receive and target reflection measurements to compensate for transmit polarization errors.

Index Terms — Calibration, phased arrays, radar polarimetry.

I. INTRODUCTION

A polarimetric radar system is able to utilize more than one polarization in order to gain information about the targets of interest by measuring its polarimetric scattering matrix S [1]. For example, weather applications utilize differential reflectivity (Z_{dr}), the ratio of reflected power in the horizontal polarization to that of the vertical polarization ($|S_{HH}|^2/|S_{VV}|^2$), to characterize the overall shape of the water droplets. Several mechanically-rotated weather radar systems already have full polarimetric capabilities [2], but they lack flexibility and are fundamentally limited in volume scan and tracking abilities.

Active phased array antennas, unlike mechanically-rotated antennas, offer rapid scanning of multiple targets with multiple receive beams and are becoming increasingly attractive for polarimetric radar applications. For example, the Multi-function Phased Array Radar (MPAR) program [3] seeks to capitalize on this idea by replacing the current WSR-88D (NEXRAD) weather radars with phased array systems that have much better update rates, the ability to track planes and weather targets simultaneously, and the capability to perform polarimetric measurements. Unfortunately, phased arrays have inherent calibration challenges. Like traditional mechanically-rotating radars, phased array radars must be calibrated initially in a controlled environment, and often the calibration itself must be monitored once the system has been installed in the field [2], [4]. Additionally, each element must be aligned in amplitude and phase, often taking mutual coupling into account [5], and the radiated power and sensitivity vary as a function of scan angle. The fundamental challenge in using phased arrays for polarimetric applications, though, is that they have polarization characteristics that change as a function of scan angle, limiting the quality of measured polarimetric data unless corrections are made [6], [7].

To investigate potential calibration procedures for mitigat-

ing this distortion in polarization caused by phased array antennas, a 10-element linear array (with 8 active and two passively terminated elements) of dual-polarized, S-band, stacked patch antennas has been connected to the Digital Array Radar (DAR) prototype [4], [8], as shown in Fig. 1. It has 16 transmit and receive channels with digitization of the signals at each polarization of each element, providing a flexible calibration testbed with full digital beamformers. Section II of this paper develops a system model and calibration procedure for the radar that focuses on being able to accurately measure and compensate for distortion as a function of scan angle, and Section III demonstrates the effectiveness of this technique by showing that accurate polarimetric measurements can be made in the presence of these distortions.

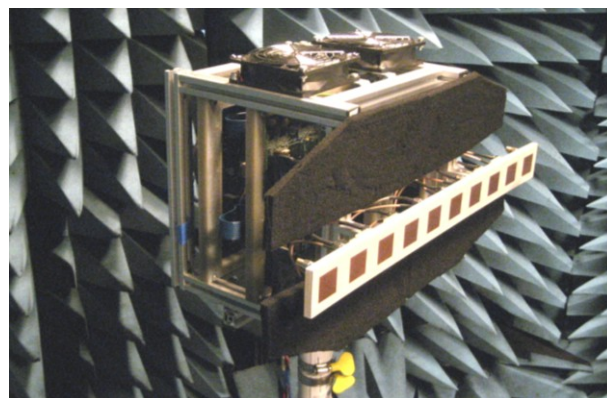


Fig. 1 Linear array of dual polarized antennas on the DAR prototype.

II. POLARIMETRIC DIGITAL PHASED ARRAY CALIBRATION

Any dual-polarized element in an array will have varying polarization characteristics as a function of the scan angle [6]. Fundamentally, this can be explained with infinite current sheets [9], the limiting case of a phased array, but a simple pair of crossed dipoles at the origin is an instructive example as well. With the horizontal (H) dipole along y -axis and the vertical (V) dipole along z -axis, the horizontal (AZ or Φ -directed) field component E_H and the vertical (EL or θ -directed) field component E_V can be expressed as [7]

$$\begin{bmatrix} E_H \\ E_V \end{bmatrix} = \begin{bmatrix} \cos(\Phi) & 0 \\ -\cos(\theta)\sin(\Phi) & \sin(\theta) \end{bmatrix} \begin{bmatrix} A_H \\ A_V \end{bmatrix}, \quad (1)$$

where A_H and A_V are the complex currents on the H and V dipoles, and the matrix is denoted as the polarimetric element pattern for the crossed dipoles. To achieve the desired polari-

zation at an arbitrary scan angle (θ, Φ) or (AZ, EL), one would have to independently adjust A_H and A_V on the dipoles by inverting the matrix in (1) and multiplying it by the desired far-field polarization. While the polarization element pattern for these crossed dipoles is simple, a generalized radiating element like the one used on the DAR prototype linear array will have a complicated one. For the n^{th} element in a phased array of generalized radiating elements, the polarimetric element pattern that takes into account imbalances and cross-couplings between the H and V radiated fields can be written as

$$\mathbf{F}_n(\theta, \Phi) = \begin{bmatrix} F_{HH}(\theta, \Phi) & F_{VH}(\theta, \Phi) \\ F_{HV}(\theta, \Phi) & F_{VV}(\theta, \Phi) \end{bmatrix}_n, \quad (2)$$

which is not known unless it is simulated or measured. Additionally, the T/R module connected to this element may have cross-coupling between its H and V ports as well as complex gain/phase imbalances between its H and V ports and those of other elements on both transmit and receive. These cross-couplings and imbalances can also be modeled by a matrix multiplication of the H and V signals presented to the T/R module on both transmit and receive with components as designated in Fig. 2. Denote this matrix for the n^{th} T/R module on transmit as \mathbf{T}_n and as \mathbf{R}_n^T on receive, where the transpose operator is included so that \mathbf{R}_n by itself has the same subscripts to its elements as the \mathbf{T}_n and \mathbf{F}_n matrices. These matrices, in the context of the DAR prototype, denote the effective complex imbalances and crosstalk from the digital beamformer input and the antenna ports on transmit and from the antenna port through the digital beamformer output on receive; the H and V chains of each and can be digitally compensated during initial alignment and calibration with individual complex weights. The matrix multiplication $\mathbf{F}_n \mathbf{T}_n$ models the effective polarization distortion from the digital beamformer all the way to the radiated far field for the n^{th} transmitter, and, due to antenna element reciprocity, the product $\mathbf{R}_n^T \mathbf{F}_n^T$ models the distortion between the incoming radiated fields and the output of the receive beamformer for the n^{th} receive element. Note that antenna elements, as seen through the T/R modules, may not be reciprocal because of the \mathbf{R}_n and \mathbf{T}_n matrices.

The overall operation of the radar with respect to polarization distortion and total antenna pattern can then be written as a matrix equation as follows, similar to the notation in [6] and [7], for a polarimetric scattering target \mathbf{S} at a particular range and angle \mathbf{r} :

$$\mathbf{V} = C \frac{e^{-2jk_0 r}}{4\pi r^2} \mathbf{R}^T(\theta, \Phi, \theta_s, \Phi_s) \mathbf{S}(r, \theta, \Phi) \mathbf{T}(\theta, \Phi, \theta_s, \Phi_s) \mathbf{A} \quad (3a)$$

$$\mathbf{R}^T(\theta, \Phi, \theta_s, \Phi_s) = \sum_n (X_n(\theta_s, \Phi_s) \mathbf{R}_n^T \mathbf{F}_n^T(\theta, \Phi)) \quad (3b)$$

$$\mathbf{T}(\theta, \Phi, \theta_s, \Phi_s) = \sum_m (Y_m(\theta_s, \Phi_s) \mathbf{F}_m(\theta, \Phi) \mathbf{T}_m) \quad (3c)$$

where $\mathbf{V} = [V_H \ V_V]^T$ is the output of the receiver's digital beamformer, C is a gain term that takes propagation loss into account, k_0 is the propagation constant, r is the distance to \mathbf{S} ,

X_n is the complex weight at the n^{th} receive port, Y_m is the complex weight at the m^{th} transmit port, θ_s and Φ_s are the current scan angles, and $\mathbf{A} = [A_H \ A_V]^T$ is the input to the transmit beamformer.

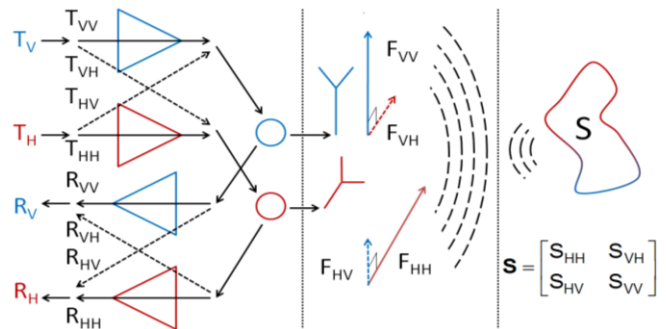


Fig. 2. Effective model for each element in an active polarimetric radar, showing the H and V signals as they pass through the T/R modules (left), the antennas (center), and scatter off the target (right).

Here, \mathbf{T} and \mathbf{R} are the overall transmit and receive polarimetric patterns, respectively, when scanned to the angles θ_s and Φ_s . Varying levels of approximation of (3) have appeared throughout the literature, including the single reciprocal antenna case [1], [6], [7], [10]. The assumptions typically made are reciprocal T/R modules and polarimetric element patterns that differ only in a phase shift due to displacement from the array origin. As discussed before, the DAR system has no guarantee on the initial reciprocity of the T/R chains before alignment, and some variation is expected in the element patterns due to mutual coupling, finite ground plane effects, and mounting hardware effects [5]. Thus, further simplifications or approximations to (3) for the DAR prototype are not made.

The goal of a polarimetric phased array radar is to accurately measure $\mathbf{S}(r_s, \theta_s, \Phi_s)$ at some scan location \mathbf{r}_s in the presence of non-idealities in the \mathbf{T} and \mathbf{R} patterns. The idea behind the compensation procedure is twofold. The first consideration is that the radar needs to provide transmit and receive patterns that have narrow beamwidths and low co-polar and cross-polar sidelobes so that only the area near \mathbf{r}_0 is interrogated, and the second is that the polarization distortion in main beams of the \mathbf{T} and \mathbf{R} patterns need to be compensated.

Synthesis of linearly-polarized patterns with low sidelobes, even in the presence of finite array effects, has been covered numerous times in the literature (e.g. [5]) and can be considered a standard phased array calibration procedure. For a simple broadside alignment which will be sufficient for the demonstrations herein, most phased array elements will have very small cross-polarization terms—perfect polarization in the case of crossed dipoles in (1)—and alignment can be performed on both polarizations at once using a slant linear polarization (equal H and V amplitude and phase) reference in an anechoic chamber. In the case of the DAR array, alignment at broadside using both a slant polarization reference and alternating H and V were tested, and they were found to give nearly identical results in off-broadside patterns. After such a calibra-

tion, the effective array factor will dominate the variation of the co- and cross-polar patterns, driving down the sidelobes of both roughly equally and leaving only significant cross-polarization and differences in co-polarization levels near the main beam.

At this point, these corruptions of polarization in the main beams of \mathbf{T} and \mathbf{R} dominate the performance of the polarimetric radar when scanning off of the principle axes, where the \mathbf{F}_n 's are usually least ideal for many element types. Corrections for these distortions can be made by characterizing the \mathbf{T} and \mathbf{R} patterns at their beam center as a function of scan angle after the alignment and calibration of the array, then applying corrections to the digital transmit and receive waveforms:

$$\mathbf{V} = C \frac{e^{-2jk_0r}}{4\pi^2} \mathbf{C}_R \mathbf{R}^T(\theta_s, \Phi_s, \theta_s, \Phi_s) \mathbf{S}(r, \theta, \Phi) \mathbf{T}(\theta, \Phi, \theta_s, \Phi_s) \mathbf{C}_T \mathbf{A} \quad (4)$$

where $\mathbf{C}_R = \mathbf{R}^T(\theta_s, \Phi_s, \theta_s, \Phi_s)^{-1}$ and $\mathbf{C}_T = \mathbf{T}(\theta_s, \Phi_s, \theta_s, \Phi_s)^{-1}$. If now \mathbf{S} is located at (θ_s, Φ_s) , the products $\mathbf{C}_R \mathbf{R}^T = \mathbf{T} \mathbf{C}_T = \mathbf{I}$ and equation (4) becomes

$$\mathbf{V} = C \frac{e^{-2jk_0r}}{4\pi^2} \mathbf{S}(r, \theta_s, \Phi_s) \mathbf{A}, \quad (5)$$

from which \mathbf{S} can be measured (to a constant) using orthogonal \mathbf{A} values, such as $[1 \ 0]^T$ and $[0 \ 1]^T$. This requires that \mathbf{R} and \mathbf{T} be measured at their beam centers at each scan angle of interest. These may be directly measured in an anechoic chamber, or target reflection-based techniques can be used, where targets with different scattering matrices train the system through calibration [10]. Specific examples of both of these are given in the next section, where these techniques are applied.

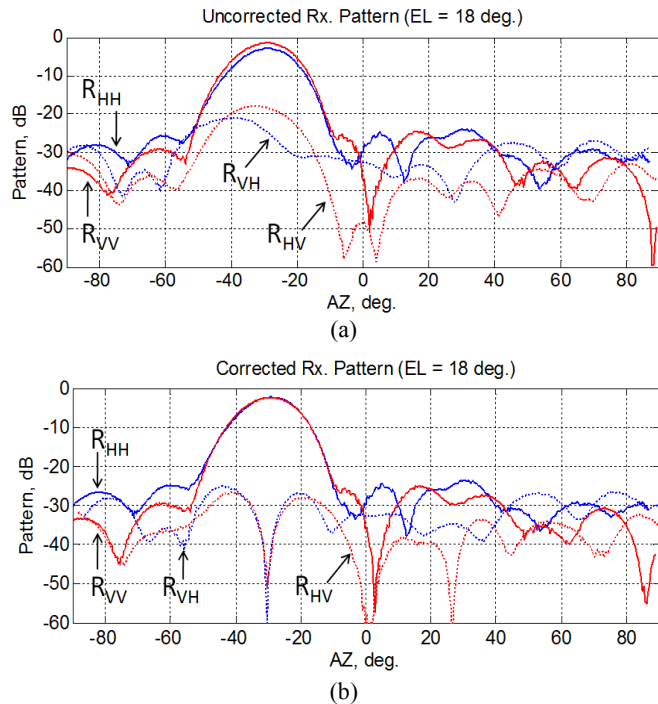


Fig. 3. \mathbf{R} pattern at EL = 18 deg., (a) uncorrected and (b) corrected.

III. DEMONSTRATION OF TECHNIQUES

The DAR testbed, shown in Fig. 1, has the capability of receiving phase-locked signals from a linearly-polarized source on each V/H channel. This permits rapid analysis of the received beam patterns \mathbf{F}_n^T of each element as well as the overall beamformer output as a function of scan angle, facilitating fast receiver alignment and characterization. For demonstration purposes, the receive elements were aligned at broadside using a slant 45-deg. linearly polarized reference (equal amplitude and phase in the H and V directions) at 3.35 GHz, and then the receive beamformer was scanned to (AZ, EL) = (-30, 18) deg. with a 30 dB Taylor weighting. This point was chosen as a representative scan angle where polarization distortion becomes significant. The subsequent pattern, the overall \mathbf{R} sum in (3), measured along the EL = 18 deg. plane, is shown in Fig. 3 before and after polarization compensation at this scan angle, which was accomplished by pre-multiplying the received waveforms by a measured value of \mathbf{C}_R from previous measurements of \mathbf{R} at its beam center when scanned at (-30, 18) deg. that had been stored in a look-up-table. The co-polarized beams initially differed by 1.5 dB at their peak, whereas the corrected beams differ by only 0.1 dB. After correction, the cross-polar main lobes were greatly diminished at the scan angle as well, and if the main beam were much narrower (for a larger array), the elimination of the cross-polar terms could likely be achieved over the entire beamwidth. Sidelobe levels were kept relatively low (~23 dB) despite the mutual coupling and mounting frame effects. This demonstrates the pattern aspects of the calibration procedure described in Section II.

Having aligned and compensated the receive side of the DAR testbed at an arbitrary scan angle of interest, making $\mathbf{C}_R \mathbf{R}$ a multiple of the identity matrix there, a procedure is now needed to measure \mathbf{T} at this location. Since reciprocity does not always apply, as discussed before, more measurements need to be made to compensate for the \mathbf{T} matrix. For the sake of demonstration, an alternative to the simultaneous direct-measurement approach used for the receivers will be used here. After aligning the transmitters at broadside, the overall \mathbf{T} matrix can be measured using target-based techniques over a range of scan angles, as done in [10]. Specifically, if \mathbf{C}_R is known at a particular scan angle and \mathbf{C}_T is initially set to be \mathbf{I} , then if \mathbf{S} is made proportional to \mathbf{I} , (4) becomes

$$\mathbf{V} = C \frac{e^{-2jk_0r}}{4\pi^2} \mathbf{T}(\theta_s, \Phi_s, \theta_s, \Phi_s) \mathbf{A}. \quad (6)$$

Two measurements made with $\mathbf{A}_1 = [1 \ 0]^T$ and $\mathbf{A}_2 = [0 \ 1]^T$ will allow direct measurements of the elements of \mathbf{T} up to an arbitrary gain constant, thus calibrating the full array at a given scan angle by calculating the \mathbf{C}_T value there and then storing it in a look-up table for future use.

As a full bi-static radar demonstration using these techniques to measure full \mathbf{S} matrices, the rightmost element is set to transmit 14 MHz wide chirped waveforms, and the four leftmost were set to receive, beamform, and match filter them

simultaneously. Only one transmit element was used since the mutual coupling values between the transmitters and the receivers was fairly high. This is all done after alignment using a slant polarization at broadside. Mutual coupling signals from the transmitter to the receivers were recorded in an empty anechoic chamber and subsequently subtracted from all receive waveforms, as in [8]. Two scan angles where polarization distortion was known to occur, specifically at (AZ, EL) = (-32, 22) deg. and (35, 17) deg., were chosen as places to introduce two targets to be measured. One was a 0.5m diameter sphere ($\mathbf{S} = S_s \mathbf{I}$) in the first location, and an array of three dipoles was placed in the second location, each about 5λ long and set next to each other at a 45 degree angle with respect to the H and V directions. This target has a nominal S matrix value of

$$\mathbf{S} = S_0 \begin{bmatrix} \cos^2(\pi/4) & \cos(\pi/4)\sin(\pi/4) \\ \sin(\pi/4)\cos(\pi/4) & \sin^2(\pi/4) \end{bmatrix} = \frac{1}{2} S_0 \begin{bmatrix} 1 & 1 \\ 1 & 1 \end{bmatrix} \quad (7)$$

The calibration target used was a $2\lambda \times 2\lambda$ flat copper sheet with ($\mathbf{S} = S_c \mathbf{I}$) placed at the locations of interest, and the corresponding \mathbf{T} (and \mathbf{C}_T) matrix values were measured using (6) and stored by scanning the 4×1 receive array in those directions while applying the appropriate \mathbf{C}_R values from the look-up-table, thus calibrating the radar.

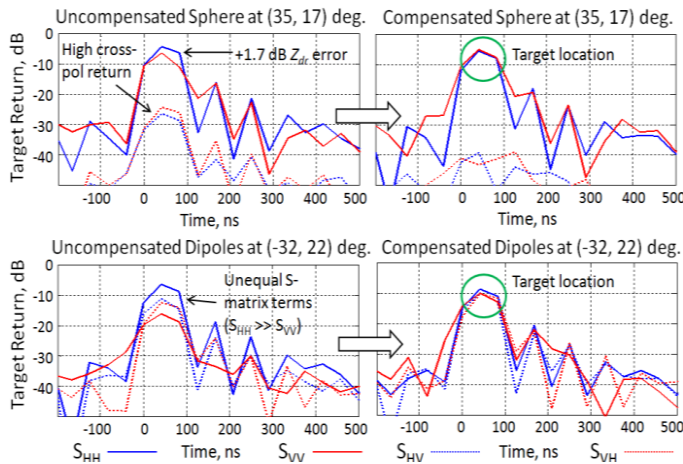


Fig. 4. Uncompensated and compensated time domain S-matrix returns for the sphere (top) and the dipole array (bottom)

The calibration sheet was removed, and the sphere was introduced at the first location to have its \mathbf{S} matrix measured by scanning the array in this direction and applying the appropriate \mathbf{C}_R and \mathbf{C}_T values. Subsequently, the sphere was removed, the array was scanned to the second location, and the dipole array was introduced in the beam and measured. The measured \mathbf{S} matrices for these targets with and without the compensation in (4) are shown in Fig. 4 in the form of their match-filtered, relative time domain magnitudes (including the time sidelobes with no windowing). Note that the time axis has an arbitrary reference close to the array face. Without compensation, the relative magnitudes of the measured

scattering matrix elements for the dipole array were significantly off of their nominal values. The 1 dB error in the corrected S_{VV} estimate the dipole array may be due to a slight deviation (~ 1.5 deg.) from 45 degrees in the relative rotation of the array. In the case of the sphere, the depolarization ratio was less than -34 dB, compared to -20 dB and the Z_{dr} error was less than 0.5 dB compared to 1.7 dB. These results indicate that the proposed technique can be effective in mitigating the effects of polarization distortion in phased arrays, even though the array used was relatively small.

V. CONCLUSION

A model for a polarimetric digital phased array radar has been presented. The calibration challenges have been outlined, and potential solutions for an active digital phased array have been demonstrated using an 8-element linear array. The practical aspects of the application of these techniques to larger arrays to obtain better polarimetric performance is a subject that warrants further study.

ACKNOWLEDGEMENT

This DAR project was sponsored by CERDEC (U.S. Army) with collaboration and contributions from Sierra Monolithics, Inc., Lockheed Martin, and CREE Semiconductor.

REFERENCES

- [1] V. Chandrasekar, R. Keeler, "Antenna pattern analysis and measurements for multiparameter radars," *Journal of Atmospheric and Oceanic Technology*, Vol. 10, 1993.
- [2] J. Hubbert, et al. "NEXRAD differential reflectivity calibration," *Geoscience and Remote Sensing Symp., IEEE 2006 Intl. Conf. on*, July 31 2006-Aug. 4 2006.
- [3] Office of the Federal Coordinator for Meteorology, "Federal research and development needs and priorities for phased array radar," FCM-R25-2006, 2006.
- [4] C. Fulton, W. Chappell, "Calibration techniques for digital phased arrays," *IEEE Intl. Conf. on Microwaves, Communication, Antennas, and Electronic Systems*, Nov. 2009.
- [5] D. Kelley and W. Stutzman, "Array antenna pattern modeling methods that include mutual coupling effects," *IEEE Trans. Ant. Prop.*, Vol. 41, No. 12, Dec. 1993.
- [6] D. Staiman, "Calibration of polarimetric phased array radar for improved measurement accuracy," *IIPS for Meteorology, Oceanography, and Hydrology, 25th Int. Conf. on*, Jan. 2009.
- [7] G. Zhang, et al., "Phased array polarimetry for weather sensing: a theoretical formulation for bias corrections," *IEEE Trans. Geoscience and Remote Sensing*, Vol. 47, No. 11, Nov. 2009.
- [8] C. Fulton, et al., "A digital array radar with a hierarchical system architecture," *IEEE MTT-S Intl. Mw. Symp. Dig.*, Jun. 2009.
- [9] A. Boryszenko, "Polarization constraints in dual-polarized phased arrays derived from an infinite current sheet model," *IEEE Ant. and Wireless Prop. Letters*, Vol. 8, 2009.
- [10] M. Whitt, et al., "A general polarimetric radar calibration technique," *IEEE Trans. Ant. Prop.*, Vol. 39, No. 1, Jan. 1991.